Numerical prediction of indoor temperature stratification

Kevin Chow* **and Arne. E. Holdø***
Narvik University College, Lodve Langesgt. 2, Postboks 385, 8505 Narvik, Norway.

ABSTRACT

In many buildings, displacement ventilation is used so that contaminants can be separated from occupied space [1, 2]. A fundamental characteristic of displacement ventilation is a layer of stratified fluid that separates the occupied zone from the contaminated zone, marked by a density gradient usually due to temperature differences in the two zones. Because buoyancy is a dominant effect in these situations, natural rather than forced ventilation is commonly used.

This paper presents a series of simulations studying the prediction of steady-state stratification in a room ventilation case. Following on from work performed by lial-Awad [3], numerical simulations coupled with a 2-equation turbulence model were employed to predict the steady-state time-averaged temperature distribution and stratification layer height in a room subject to two momentum sources at different temperatures. The room has been simulated with different levels of idealism to examine the effect boundary condition assumptions have on the predictive accuracy of the simulation compared to the work of lial-Awad [3].

It was found that the assumption of adiabacity of the room caused the predicted vertical temperature profile to be highly idealistic, with the flow stratified into two discrete layers across a sharp interface. The addition of heat loss boundary conditions and thermal radiation modelling causes the predicted temperature profile to more closely match that produced in the original experimental work.

Keywords: RANS, ventilation, stratification

1. INTRODUCTION

Room ventilation flow is a well studied area, as there is an ever-growing desire to utilise natural methods for their ventilation in order to reduce the expenditure in air conditioning and ventilation systems, reducing energy costs and also preserving the environment.

Natural ventilation uses fluid buoyancy to ventilate interiors, driven by temperature gradients inside the structure, as well as any external forcing such as wind. A technique which uses, or works in conjunction with natural ventilation, is displacement ventilation. Displacement ventilation (DV) involves the establishment of a stratified layer with a warm, buoyant, contaminant fluid above, and colder, less buoyant fluid below. Cold air is supplied at the lower level, and used/contaminated air is convected up in buoyant plumes driven by heat sources. Air at the upper level is exhausted, encouraging a vertical convection which

*Corresponding author: chowk9@coventry.ac.uk. Tel.:+44 24 7688 8928
*Professor Arne E. Holdø -Tel.:+44 24 7688 8792 (direct) E-mail: arnhol@hin.no

constantly refreshes air in the lower level and exhausting them out at the upper level. The opposite method, mixing ventilation, is characterised by a mixing of the two (or more) zones by depositing negatively buoyant fluid above the buoyant fluid. This stops the formation of a stratified layer, and the constant upheaval of buoyant and negatively-buoyant fluid causes continual ventilation.

Displacement ventilation is useful in inhabited spaces, as the stratified layer makes it possible to restrict contaminants, or air at undesirable temperatures, to certain areas inside the building – mixing ventilation may not be as suitable, or not as efficient as DV. DV also dispenses with the need to actively ventilate the enclosure with air at high velocities, which reduces comfort. The existence of the stratified layer is crucial to DV, and the strength of the stratified layer can be described by the ratio of buoyant and inertial forces using the Richardson number:

$$Ri = \frac{g'h}{u^2} \tag{1}$$

Where g' is the reduced gravity parameter defined by $g' = g\frac{(\rho_1 - \rho_\infty)}{\rho_\infty} = g\frac{(T_1 - T_\infty)}{T_\infty}$ for an ideal gas; h is the characteristic length and u^2 is the characteristic velocity scale. Richardson numbers as low as 0.25 have been shown analytically to be capable of sustaining stable layers [4].

Calay et al. and Skistad [5, 6] experimentally combined displacement ventilation with partitions at the stratification height in order to divide the working space into a series of zones in order to account for the ventilation requirements of each contaminant zone, in a principle called “selective withdrawl”. This partitioning allows the ventilation of each zone to be specifically tailored to increase local efficiency but also allowing the floor level to be unobstructed. One observation they noted was the ability for selective withdrawal methods to operate in temperature gradients as low as 0.125°C/m.

Using a number of experiments inside rooms of moderate heights of 2.4 to 2.7m, Mundt [7] found that the temperature gradient is dependant on the ventilation rates, and that the actual location of the heat sources and thus the heat load distribution affected the gradient to a lesser degree. This is likely due to be because the ratio of plume diameter against the width of the room is of a similar order; in a larger room, plume effects could lead to local conditions that differ elsewhere in the room.

A great deal of work has been done by Linden and his co-workers on natural ventilation, and the formation of simple models to determine interface heights, effective areas and distributions [2, 8, 9] of temperature. One critical aspect of natural and displacement ventilation is the neutral layer height. In natural ventilation cases where an opening to the external environment exists, the neutral layer height is determined by the surroundings, which has a linear variation in vertical hydrostatic pressure dp/dz; in this case, the neutral layer occurs when the internal pressure gradient intercepts the external pressure gradient.

In displacement ventilation, the wall temperature is the defining parameter. Here, the neutral layer occurs at the intercept of the vertical temperature profile with the mean vertical wall temperature [10, 11]. The flow into and out of the space is controlled, but exhaust vents must be carefully located above the neutral layer to ensure that the contaminated (upper) zone is efficiently removed.

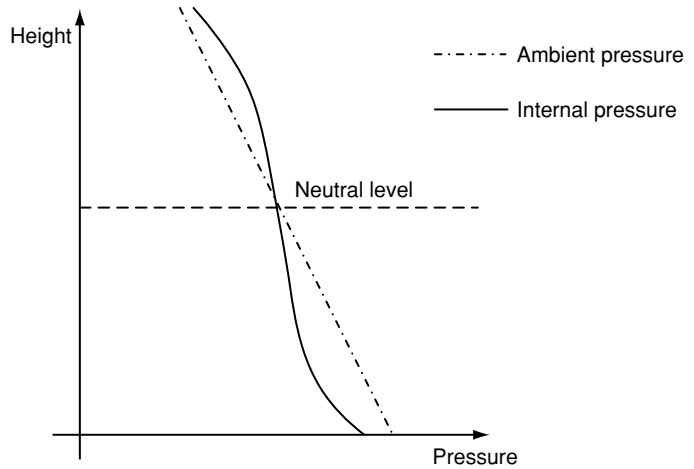

Figure 1 Plot of neutral layer determination by internal pressure relative to ambient.

2. RADIATIVE EFFECTS

In recent years, the effect of radiant thermal transfer on natural ventilation situations has been under more scrutiny, as the increasing affordability of high-performance computing allows the solution of the radiative heat transfer equation, as well as more complex radiation models.

Air participates in radiation transfer due to its concentration of water vapour and, to a lesser extent, carbon dioxide. Both gases have resonant bands which absorb and emit infrared radiation.

Although it was common practice to ignore radiative heat transfer in small enclosed structures, some authors, for example Howell and Potts [12], and Kondo et al. [13], have begun integrating radiative heat transfer in their predictive models. Howell and Potts noted that previous experimental work involving salt baths, where densimetric stratification occurs through density differences from the salt content, does not account for radiative transfer, and also salt water has a lower level of molecular diffusivity, so that stratified interfaces are much sharper.

Li et al. [14] surmised that the effect of radiative transfer in applications using displacement ventilation is that radiative heat not only warms up the air, but also warms up the walls, which also transmits heat to the surrounding air. This reduces the temperature gradient across the stratified layer, reducing the buoyancy flux across it. This reduction in flux reduces the efficiency of the ventilation, which relies on a strong pressure differential to drive the stratification process. These results can be seen graphically in Li's data, as well as Howell and Potts' data [12]. In comparison, the experimental data by Hunt et al. [9] shows a very sharp gradient between the stratified layers.

Glicksman and Chen [15] performed CFD and analytical analyses of heat transfer to examine the impact of radiative heat transfer. They observed that as radiative transfer depends on the path length and absorptivity, overall heat transfer by radiation does not affect the distribution in small enclosures, but is increasingly important as the enclosure size increases, optical thicknesses go up (due to increasing path length) and the radiating surface area increases.

Most of the authors who studied conjugate heat transfer assumed that water vapour was the only participating gas in air. Carbon dioxide, which is present in much lower quantities also plays a part in radiation. Between them, water vapour has a Planck-mean absorption of around

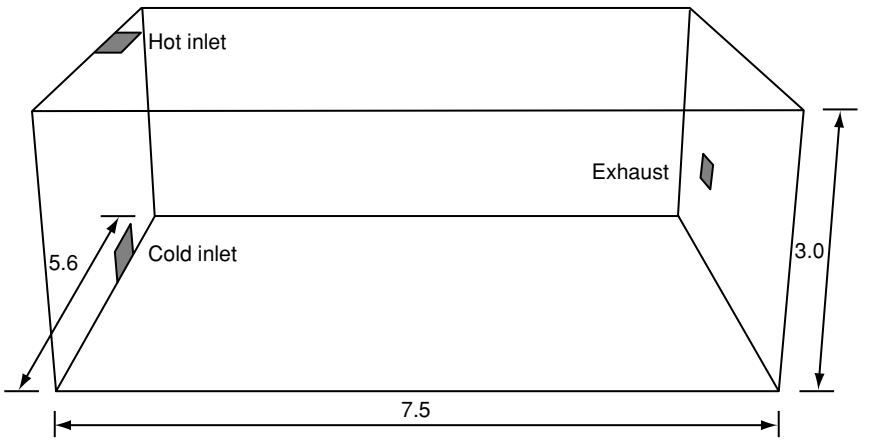

Figure 2 Schematic of environmental chamber geometry.

$0.17m^{-1}$ and carbon dioxide somewhere around $0.08m^{-1}$. However, it is known that both H_2O and CO_2 share common resonance bands, the primary one being at 2.7 microns, which reduces the overall emission due to increased self-absorption of emitted radiation [16].

3. DESCRIPTION OF MODEL

The simulated domain is geometrically similar to the experiments performed by Iial-Awad, who examined the stratification of a room subject to multiple heat and momentum fluxes. The work was carried out using the whole environmental chamber at the University of Hertfordshire, of dimensions given in Figure 2.

Three momentum inlets exist, supplying air at different flow rates and temperatures. A cold air supply is located at floor level, supplying air at the external ambient air temperature. A hot air supply is located at the ceiling, blowing down, supplying air at 45C. Another cold air supply is located in the centre of the ceiling, of area $0.11m^2$, to supply a high momentum jet into the chamber. A single exhaust is located on the far wall placed at half-height. All vents are covered by a 10mm-square mesh which negates any non-uniformity in the flow, and also imposes uniform turbulent conditions at the exit face.

The chamber walls are constructed of a polyurethane foam sandwiched by a thin polyester finish with a total thickness of 125mm. The floor consists of 100mm concrete atop an additional thickness of 100mm of polystyrene tiles.

4. NUMERICAL MODELS

The simulation was performed using the commercial computational fluid dynamics package Fluent 6.2, which solves the Navier Stokes equations to describe complex fluid flow:

$$\frac{\partial(\rho u)}{\partial t} + u_j \frac{\partial(\rho u_i)}{\partial x_j} = -\frac{\partial p}{\partial x_i} + \frac{\partial}{\partial x_j}\left(\nu\left(\frac{\partial u_i}{\partial x_j} + \frac{\partial u_j}{\partial x_i}\right)\right) + \rho g + F \tag{2}$$

Where ρ and u are the density and velocity terms respectively, and ν is the kinematic viscosity; F is an additional source term. Although the differential form is given here, the integral form is solved in the software, and so mass is automatically conserved. Essentially,

the time rate of change of momentum and acceleration terms result in changes in pressure and viscous effects. The buoyancy term ρg is added as an extra source term in the Navier-Stokes equations. Although use of the Boussinesq approximation in calculating buoyant flows is common, it was not used here due to the use of other numerical models (such as radiation) which require the calculation of flow energy. Instead, the ambient fluid model was modelled as an incompressible gas.

Heat and energy transfer is accounted for using the conservation of energy:

$$\frac{\partial(\rho e_i)}{\partial t} + \frac{\partial(\rho u_j e_i)}{\partial x_i} = \frac{\partial}{\partial x_j}\left(k\frac{\partial T}{\partial x_j}\right) \tag{3}$$

Where e is the internal energy, k is the conductivity of the volume and T is the temperature.

The equations were solved on finite volume meshes using a third-order MUSCL [19] (Monotonically Upstream-centred Scheme for Conservation Laws) discretisation scheme to reduce numerical loses, such as numerical diffusion which can smear results. The PISO method [19] of pressure linking is used to minimise the effect that any skewed cells in the mesh have on the accuracy and stability of the simulation.

Fluid turbulence occurs at Reynolds numbers of 10,000 or more, and causes significant changes in the behaviour of the flow, for example the rate of mixing, which in areas of high turbulence, increases by several orders of magnitude over mixing caused by molecular diffusion alone. In the simulations presented, turbulence was modelled using the two-equation realizable K-Epsilon model from Shih et al. [19], which uses a different formulation for the eddy viscosity calculation, as well as making the turbulent viscosity coefficient variable depending on the mean flow vorticity, shear and local turbulence conditions. A new expression for the dissipation rate equation has been derived and found to predict the spreading of round jets much more accurately.

The calculation of radiative effects was carried out using an implementation of the Discrete Ordinates model over a finite volume scheme [20], which solves the radiative heat transfer equation over a finite number of solid angles.

It is well known that other models, such as the P-1 approximation and Rosseland models work well in applications where the multiple of absorption coefficient and path length $\alpha\ell$, or optical thickness, is high, partly due to the assumption of isotropic radiated energy [16]. However in this case, the participating media, air, has a low absorption coefficient, so that the overall optical thickness is below the range in which both of the former models give accurate approximations.

5. BOUNDARY CONDITIONS

In the model, three simulations were conducted on the assumption of adiabacity and negligible heat transfer through radiation, at different flow rate conditions as shown in Table 1.

Following on from this initial work, additional boundary conditions were added to Case 3 to account for heat loss through the walls floor and ceiling, and then radiative heat transfer.

A uniform heat loss was modelled on all of the walls, with all walls having a calculated fixed U-value of 0.162W/m^2 based on material specifications given by Iial-Awad and heat transfer values from Bejan and Krause [21], compared to the U-value of 0.186W/m^2 calculated by Pikos [22].

Radiative boundary conditions assumed emissivities of 0.9 for all boundary walls, and an absorption coefficient of 0.049 was used for air with low relative humidity.

Table 1 Simulated cases and associated boundary conditions

	Hot inlet m/s (m^3/h)	Cold inlet m/s (m^3/h)	Hot inlet Temp C (K)	Cold inlet Temp C (K)
Case 1	0.2 (3)	0.067 (2)	45 (318)	27 (300)
Case 2	0.2 (3)	0.2 (6)	45 (318)	27 (300)
Case 3	0.13 (2)	0.2 (6)	45 (318)	23 (296)

6. RESULTS

Figure 4 to Figure 6 show the temperature distribution inside the chamber for cases 1 to 3, in comparison to the experimental results of Iial-Awad [3].

The inlet Reynolds numbers are low, below 1×10^4, resulting in low levels of turbulence in the domain, which are further decayed across the stratified layer, reducing vertical transfer [23]. The decay of turbulence can be seen particularly clearly on the adiabatic model. The resulting strong stratification by the idealised models gives rise to a steep gradient.

The resulting Richardson numbers across the adiabatic cases is fairly constant due to the similar temperature profiles, resulting in $Ri \approx 8$ (Figure 6). With the introduction of heat transfer across the walls and internal radiation between the air and the walls (Figure 9), and external radiative emission out of the system, the temperature gradient weakens, resulting in a Richardson number of 2 which contrasts well with a value of 1.1 from the results of Iial-Awad.

The mesh sensitivity of the case was also studied (Figure 3) based on three different mesh sizes from 400,000 to 800,000 cells using the boundary conditions from Case 3 without the assumption of adiabacity as a reference. All results are fairly similar and well within 1 degree of each other across the entire range, showing that the mesh sensitivity does not play a large factor in the outcome of the simulation. On a more practical level, the convergence of the 400,000 cell mesh proved difficult because of the larger gradients through cells and the overall coarseness near momentum sources. As the 800,000 cell mesh is also more computationally intensive due to the sheer number of extra cells, the 600,000 cell mesh was used for the rest of the predictions.

Following on from initial simulations using full assumptions of negligible heat loss and radiation, these assumptions were removed one by one using boundary conditions described above, yielding results as given in Figure 9, where it can be seen that the effects of the different levels of assumptions have a profound effect on the prediction of the temperature profile.

7. DISCUSSION

Figure 4 to Figure 6 clearly show that the predicted temperature profile on the assumptions of adiabacity and negligible radiation is highly idealised in comparison to the experimental results, essentially resembling a step change in temperature. The experimental results shown in Figure 4 and Figure 5 both have a fairly strong temperature gradient near the floor, as well as another slight “kink” in the temperature profile between 1m and 2m, which is not predicted by either model. As none of the walls are subject to heat or radiative fluxes, the temperature distribution is determined by the momentum fluxes and the interface level by the vertical pressure distribution.

Numerical simulation work by Pikos [22] showed that for a fixed momentum flux into the chamber, varying the vertical location of the exhaust height affects the location of the stratified layer. This is expanded upon by Iial-Awad, who noted that when the flow is momentum-dominated (low ratio of cold to hot inlet flow rates), the exhaust height has a minimal influence on the interface height, but when buoyancy forces are high the exhaust vent can “attract” the stratified layer towards it [3].

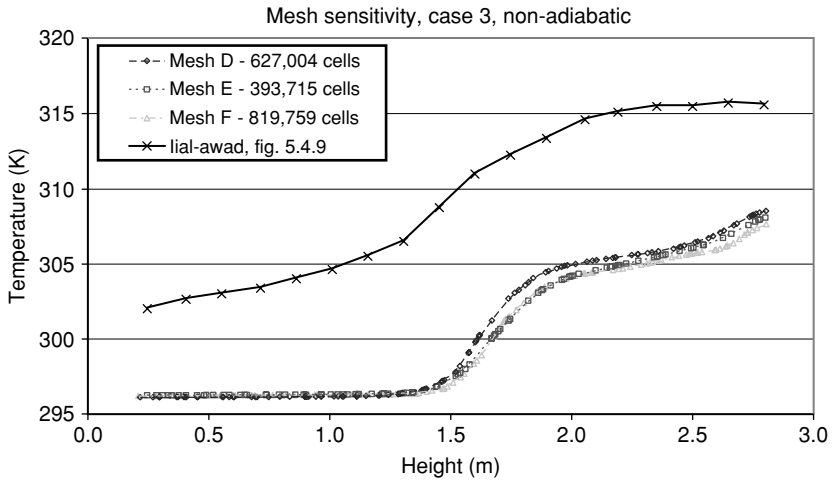

Figure 3 Mesh sensitivity testing of three different meshes.

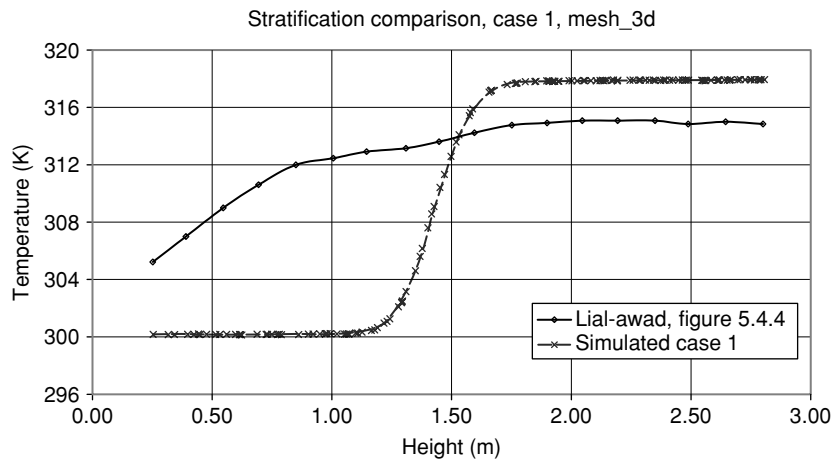

Figure 4 Simulated versus experimental results from Case 1 conditions.

7.1. EFFECTS OF ADIABACITY

The assumption of adiabacity has a profound effect, as without heat loss the temperature stratifies into two regions whose temperatures are governed by the inlet temperatures, and the layer height determined by the vertical pressure profile. Without being able to lose heat to the surroundings, heat can only transfer between the stratified layer. However, due to the low turbulence conditions and the strength of the stratified layer, heat transfer between the layers is primarily through conduction and limited vertical transport through the layer itself.

With the addition of heat loss boundary conditions, the maximum temperature is greatly reduced due primarily to loss through the ceiling; the lower zone is unaffected, as heat transfer to the lower zone still relies on transfer through the stratified layer. The thickness of the interfacial layer remains roughly constant, as does its location.

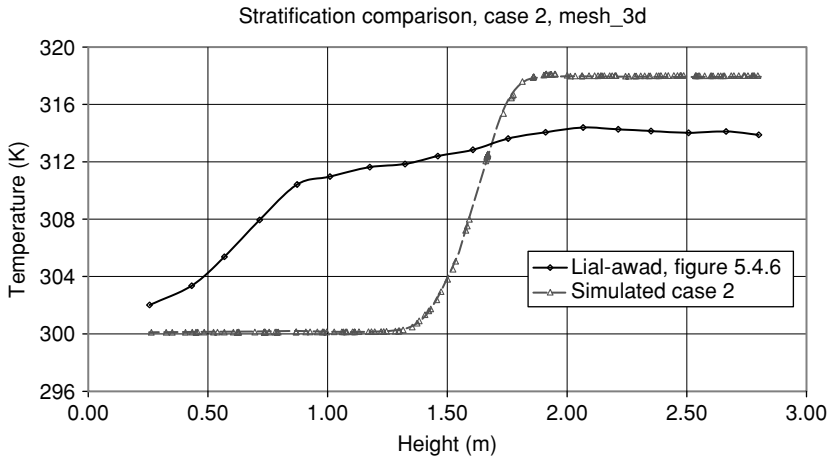

Figure 5 Simulated (dashed) results versus experimental (solid) results from Case 2.

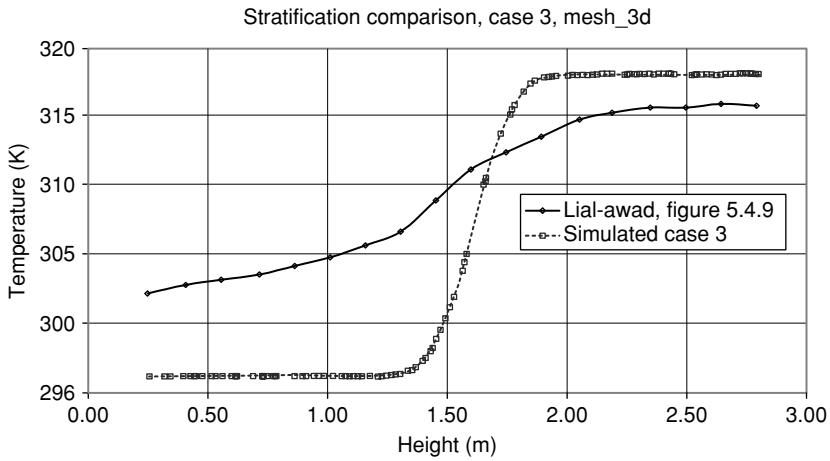

Figure 6 Simulated versus experimental results from Case 3 conditions; note all simulations have a very simple temperature profile.

7.2. EFFECTS OF RADIATIVE HEAT TRANSFER

The main influence of radiation is through the heating of the chamber walls, which both emit and conduct heat back into the surrounding air. As the chamber has a relatively fairly thin optical thickness, radiation absorption and emission from the air itself does not have such a large impact on the temperature profile, although the joint effects are enough to raise the temperature of the air by around two degrees. The primary path of radiative transfer is from the upper zone to the lower; although the ceiling is primarily an emitter and the floor and absorber, the side walls also play a part as dictated by their wall temperature (Figure 10).

There is a difference in the temperature profile in the cold region; with the application of radiation, the cold region is no longer at a constant temperature up to the stratified region; instead, the radiation has radiated down from the upper zone through the stratified layer and increased the temperature of the lower zone. This is similar to the phenomena exhibited by Li, et al. [14] where the effect of radiation is to heat the floor and lower zone, potentially decreasing the temperature gradient across the stratified layer, weakening it.

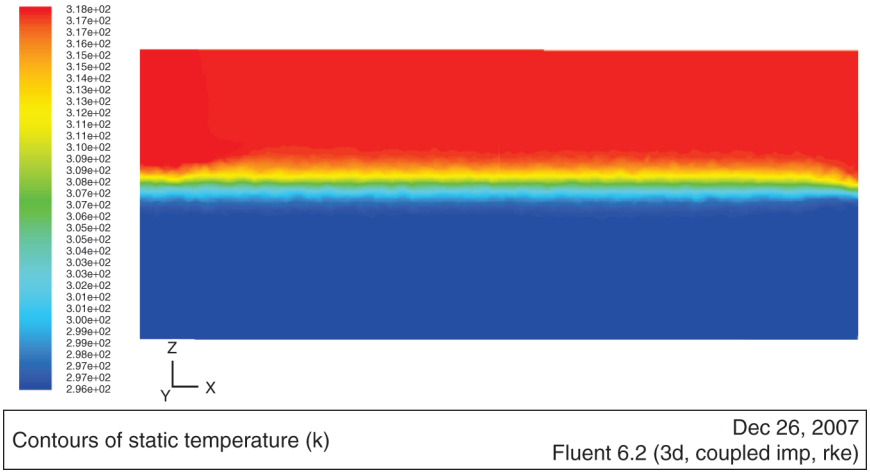

Figure 7 Temperature plot of adiabatic simulation; inability of heat to escape from system creates a strong stratification.

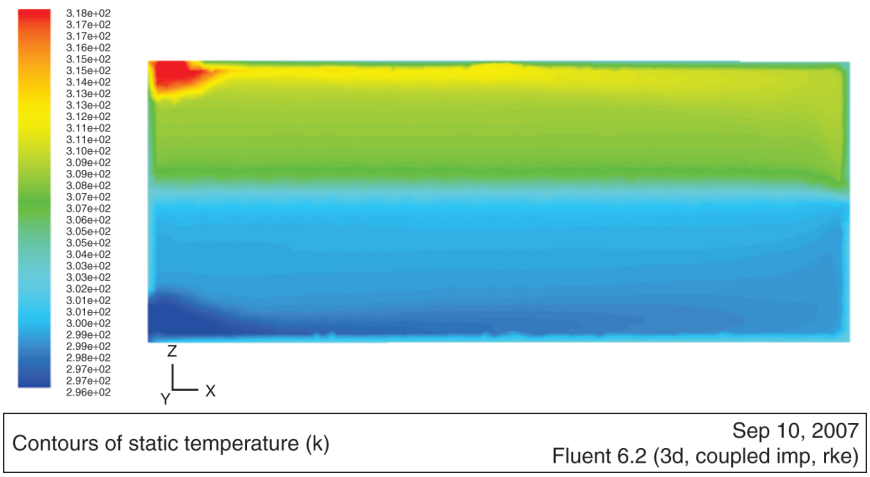

Figure 8 Temperature contour plot of full simulation; temperature bounds are different, and temperature profile is less steep.

7.3. TEMPERATURE DEFECT

Although the trends of the results of the more complex simulations show a marked increase in accuracy to the experimental results over the adiabatic simulations, there remains a large gap of around 6 degrees between the boundary temperatures compared to the experimental results. There are a number of possibilities as to why, but it is difficult to mitigate them.

The experimental results were carried out over long periods of time during the summer season in the UK. Because the time required to achieve steady state results can be a number of hours, the conditions outside of the chamber are bound to change as the external conditions and the outside weather change. As the cold air supply was taken from the ambient air, the temperature and humidity varied as did the surroundings. Again, as

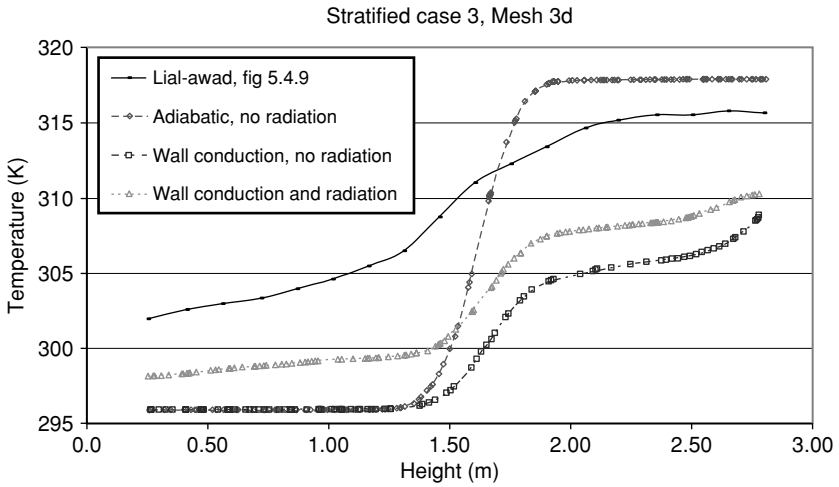

Figure 9 Comparison of various simulations using Case 3 conditions with varying assumptions.

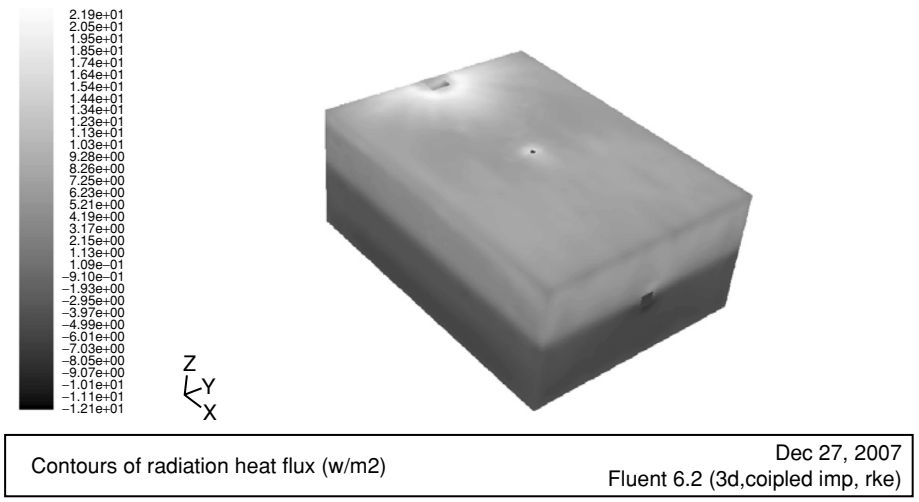

Figure 10 Radiative heat flux of enclosure.

the experiments were conducted during the summer season, the peak temperatures could have been higher than the stated values. As they were not recorded, accurate replicate of the experimental conditions is very difficult.

One area which can greatly affect the heat transfer through the chamber walls is the external wall temperature. Because the external wall temperatures were not recorded, an accurate wall temperature cannot be given which leads to heat loss effects being inaccurate, which then affects the air temperature inside the domain, as well as affecting the prediction of the neutral layer. The wall temperature will vary in height, leading to slightly more heat loss through the ceiling, and less towards the floor in the lower zone, resulting in higher lower-zone heating.

8. CONCLUSIONS

The effects of different physical assumptions have been examined with respect to indoor ventilation prediction using numerical simulation. It was found that while adiabatic heat transfer obviously results in a highly idealised result, the addition of radiative models was more subtle; increased internal heat transfer due to radiation resulted in an increase in internal air temperatures.

The addition of a radiative transfer model increases the temperature due to emission and re-absorption of radiated heat, primarily by the walls due to the low optical thickness. Primary radiative mechanisms involve the hot ceiling warming the floor, confirming that as seen in other work [12–15].

REFERENCES

[1] Linden, P. F., The Fluid Mechanics of Natural Ventilation, *Annual Review of Fluid Mechanics*, 1999, **31**: 201–238.

[2] Holford, J. M., Hunt, G. R., Fundamental Atrium Design for Natural Ventilation, *Journal of Building and Environment*, 2001, **38**:409–426.

[3] Iial-Awad, A. S., *Stratified Flow in the Built Environment*, Ph. D. Thesis, University of Hertfordshire, United Kingdom, 2006.

[4] Miles, J. W., On the stability of heterogeneous shear flows, *Journal of Fluid Mechanics*, 1961, **10**:496–508.

[5] Calay, R. K., Borrensen, B. A., Holdo, A. E., Selective Ventilation in Large Enclosures, *Journal of Energy and Buildings*, 2000, **32**:281–289.

[6] Skistad, H., Utilizing Selective Withdrawal in the Ventilation of Large Rooms: Select Vent, *Roomvent 1998 - the 6th International Conference on Air Distribution in Rooms*, Stockholm, Sweden, 1998.

[7] Mundt, E., Displacement Ventilation Systems - Convection Flows and Temperature Gradients, *Building and Environment*, 1995, **30**:129–133.

[8] Linden, P. F., Lane-Serff, G. F., Smeed, D. A., Emptying filling boxes: the fluid mechanics of natural ventilation, *Journal of Fluid Mechanics*, 1990, **212**:309–335.

[9] Hunt, G. R., Cooper, P., Linden, P. F., Thermal Stratification Produced by Plumes and Jets in Enclosed Spaces, *Journal of Buildings and Environment*, 2001, **36**:871–882.

[10] Stymne, H., Sandberg, M., Mattsson, M., Dispersion pattern of contaminants in a displacement ventilated room - implications for demand control, *12th AIVC Conference - Air Movement & Ventilation Control Within Buildings*, Ottawa, Canada, 1991, 173–189.

[11] Xing, H., Awbi, H. B, Measurement and calculation of the neutral height in a room with displacement ventilation, *Journal of Building and Environment*, 2002, **37**:961–967.

[12] Howell, S. A., Potts, I., On the natural displacement flow through a full-scale enclosure, and the importance of the radiative participation of water vapour content of the ambient air, *Building and Environment*, 2002, **37**:817–823.

[13] Kondo, Y., Ogasawara, T., Fujimura, J., Interactive Simulation of Room Air Temperature and Absorption/Emission of Radiative Heat with Room Moisture, *Roomvent 2000 - 7th International Conference of Ventilation for Health and Sustainable Environment*, Reading, United Kingdom, 2000.

[14] Li, Y., Sandberg, M., Fuchs, L., Effects of thermal radiation on airflow with displacement ventilation: an experimental investigation, *Energy and Buildings*, 1993, **19**:263–274.

[15] Glicksman, L. R., Chen, Q., Interaction of Radiation Absorbed by Moisture in Air with other forms of Heat Transfer in an Enclosure, *Roomvent 98 - 6th International Conference on Air Distribution in Rooms*, Stockholm, Sweden, 1998, 111–118.

[16] Modest, M. F., *Radiative Heat Transfer*, 2nd Ed. Academic Press, 2003.

[17] van Leer, B., Towards the Ultimate Conservative Difference Scheme. V. A Second-Order Sequel to Godunov's Method, *Journal of Computational Physics*, 1978, **32**:229–248.

[18] Issa, R. I., Solution of Implicitly Discretized Fluid Flow Equations by Operator Splitting, *Journal of Computational Physics*, 1986, **62**:40–65.

[19] Shih, T-H., Liou, W. W., Shabbir, A., Yang, Z., Zhu, J., A New K-E Eddy Viscosity Model for high Reynolds Number Turbulent Flows, *Computers and Fluids*, 1994, **24**(3):227–238.

[20] Chui, E. H., Raithby, G. D., Computation of Radiant Heat Transfer on a Nonorthogonal Mesh using the Finite-Volume Method, *Numerical Heat Transfer*, 1993, **23**:269–288.

[21] Bejan, A., Kraus, A. D., *Heat Transfer Handbook*, John Wiley & Sons, 2003.

[22] Pikos, K., *The stability of stratified layers within ventilated enclosures*, Ph. D Thesis, University of Hertfordshire, United Kingdom, 2006.
[23] Fernando, H. J. S., Turbulent Mixing in Stratified Fluids, *Annual Review of Fluid Mechanics*, 1991, **23**:455–493.